Observation of Nonlinear Acoustic Effects in a *B*-Scan Imaging Instrument

KEVIN J. PARKER, MEMBER, IEEE

Abstract—**Finite amplitude distortion in acoustic waves can be produced by a commercial *B*-scan imaging instrument which has an unconventionally long water delay path. The presence of harmonic signal components at high power output is compared to theoretical predictions, and the significance of these findings are discussed. It is shown that imaging properties are not noticeably affected under the weak shock ($\sigma = 1$) conditions.**

Introduction

IT IS WELL-KNOWN that finite amplitude effects can occur in water at biomedical frequencies and intensities [1]–[4], and the production of finite amplitude distortion in pulsed fields from diagnostic ultrasonic equipment has recently received attention [5]–[6]. The distortion of a propagating pure tone wave can be characterized, in the time domain, by the formation of a "sawtooth" wave appearance, or in the frequency domain by the generation of harmonics. A shock parameter σ provides a useful characterization of these effects, with $\sigma = 1$ representing weak shock, and $\sigma = 3$ indicating mature hard shock [1]. The magnitude of σ is related to the nonlinear parameter B/A of the medium, to the propagation distance through the medium, and the source intensity and frequency. Thus an ultrasonic instrument using a combination of high source intensities, high frequencies, and long water delay paths may be capable of operating in the $1 < \sigma < 3$ region of shock wave production. This is undesirable for a number of reasons. From a safety standpoint, interactions and potential bioeffects of shock waves on tissue are not well described. From imaging considerations, the production of shock waves can cause a saturation effect [1], where increasing source intensities do not produce corresponding increases in field intensities. Beam patterns can be enlarged [2], degrading lateral resolution. Finally, any energy converted to higher harmonics is lost to the effects of higher attenuation in media and signal rejection by band-limited transducers and receiver amplifiers. This could lead to a decreased penetration depth in an imaging system. The material presented herein illustrates the onset of weak shock conditions in a clinical *B*-scan instrument.

Methods

The *B*-scan instrument used in this study was the Octoson (Ausonics, Ltd., Australia) which features eight independent 3-MHz center frequency transducers of approximately 70-mm diameter, focused at a distance of 355 mm. Compared to the majority of ultrasonic imaging systems, the Octoson features an unusually long focal length and large water delay line between transducers and targets. This provides a useful flexibility in clinical and scientific studies [8], but is also a critical factor in the generation of finite amplitude effects. The Octoson rubber membrane used for clinical studies was removed from the water bath surface for the purposes of this study, and a Saran Wrap coupling bag filled with approximately 2 cm of water and 2 cm of castor oil was placed in contact with the Octoson water bath. A hydrophone was inserted through the castor oil layer, which served as an acoustic absorber, and was positioned in the water layer. The hydrophone was a 1-mm diameter polyvinylidene fluoride (PVDF) receiver (Medicoteknisk Institut, Denmark), having a flat frequency response between 1 and 10 MHz [9]. The probe was located approximately 10 mm proximal to the nominal focal region (at 345 mm from the transmitter) for these studies and was carefully aligned to maximize the received signal within the converging beam. The hydrophone output was directly connected to an oscilloscope, and the amplified oscilloscope output was connected to a spectrum analyzer. A single transducer was made to continue pulsing while remaining stationary, through selection of "M Mode" operation. The acoustic power output of the transmitter was adjusted by changing the "dB" setting on the Octoson controls, variable in 1-dB increments between 0 (lowest) and 45 (highest) dB. The experiments were performed in a water bath temperature of 35 °C, which is the normal operating temperature for the Octoson. A "tissue equivalent" phantom (backscatter, sound speed, and attenuation similar to values found in soft tissue) from RMI Corporation (Middleton, WI) was used to evaluate images at varying power levels.

A separate test of receiver, amplifier, and spectrum analyzer linearity was also made to ensure that any observed distortions were generated in the water and did not represent measurement artifacts. In these tests, the PVDF hydrophone was again connected through the oscilloscope amplifier to the spectrum analyzer, and was located 1 cm from the surface of a 2.5-cm diameter, 1 MHz, ceramic transducer. The short propagation path from transmitter to receiver eliminates the possibility of shock wave formation for intensities below 50 W/cm^2. The transducer was driven at 1 MHz and later at 3 MHz by a power am-

Manuscript received December 7, 1983; revised August 3, 1984. This work was supported under Grants from the Whitaker Foundation and the United States Public Health Service (GM-09933).

The author is with the Department of Electrical Engineering, University of Rochester, Rochester, NY 14627, USA.

0018-9537/85/0100-0004$01.00

plifier with controllable gain. Linearity was determined by plotting the increase in received signal, measured on the spectrum analyzer, for known increases in radio frequency (RF) voltage applied to the transducer. The test system remained linear at both 1 and 3 MHz to a receiver level of 50 dB above noise, where second and third harmonic components were first noted.

In comparison, waveforms from the Octoson were measured at 0 to 30 dB above noise, well within the linear range of the hydrophone spectrum analyzer combination.

Theory

For spherically converging waves propagating in a nonattenuating medium, the shock parameter is defined by [1], [10]

$$\sigma = \beta \epsilon k R \ln(R/r) \tag{1}$$

where R is the effective radius of the spherical source, r the distance from the center of curvature, k is the acoustic wavenumber, and

$$\beta = 1 + B/2A \tag{2}$$

$$\epsilon = (2 I_s \times 10^7 / \rho c^3)^{1/2}. \tag{3}$$

In the above expressions, I_s is the rms source intensity (W/cm^2), and ρ and c are the density and sound speed of the medium in CGS units [1]. Using typical values for a water medium with $B/A = 5.2$, $\rho = 1$ gm/cm^3, and $c = 1.5 \times 10^5$ cm/s, (1) becomes

$$\sigma = 1.161 \times 10^{-8} f R \ln(R/r) (I_s)^{1/2} \tag{4}$$

where f is the fundamental frequency. Equation (4) shows that, for any fixed frequency, focused transducer, and source intensity, the shock parameter will grow larger as a propagating wave nears the focal region (as r grows smaller). Where $\sigma = 1$, the distortion can be classified as weak shock, where the fundamental has lost 1 dB to harmonic generation, and the second and third harmonics are 8 and 15 dB below the fundamental [1]. To characterize the experiments reported herein, we assume that $R = 35.5$ cm corresponding to the lens focal length, $r = 1.0$ cm, and $f = 3.1 \times 10^6$ Hz. Under these conditions, (4) shows that a source intensity of approximately $I_s = 0.05$ W/cm^2 will produce weak shock conditions, $\sigma = 1$, at the observation point. Changing the values of R/r to 36.5 cm/2.0 cm yields a source intensity of $I_s = 0.07$ W/cm^2 when $\sigma = 1$. Thus weak shock conditions can theoretically be produced in the Octoson water delay tank, at locations near the focal region, when the source intensities are on the order of 50–70 mW/cm^2.

Results

No evidence of finite amplitude effects was observed over a wide range of transmit power levels commonly used for clinical examinations. However, at the highest 5 dB range of power output, the second and third harmonic signals were observed. Fig. 1 shows a spectrum analyzer display of the received signal, where the transmitted power

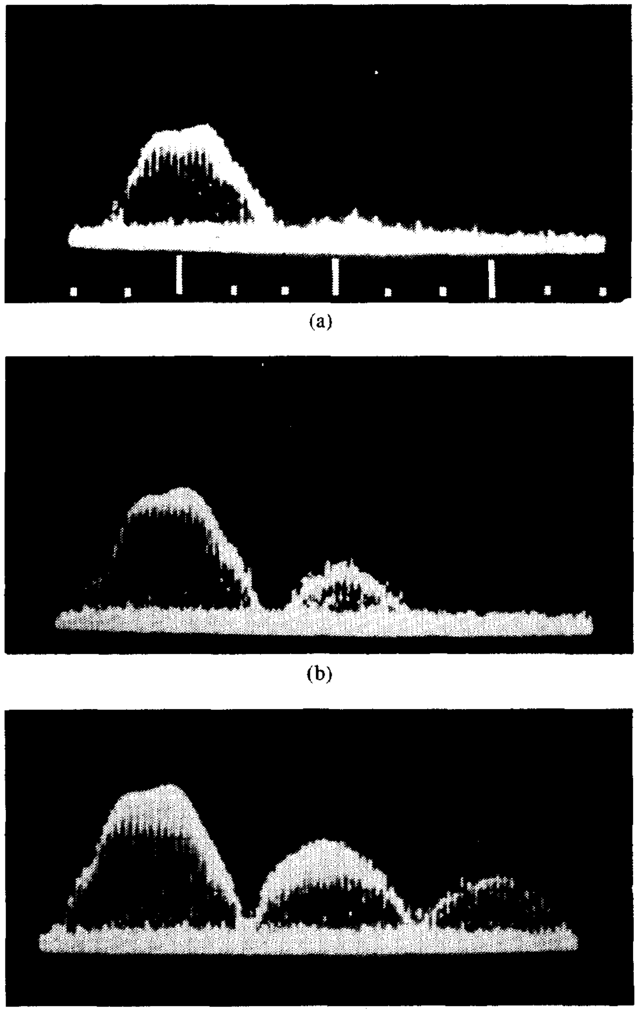

(a) (b) (c)

Fig. 1. Spectra of received signal near focal region. Horizontal scale: 1 MHz/div. Vertical scale: 10 dB/div. White marker lines indicate 3.0,6.0, and 9 MHz. Spectra are obtained for output levels of (a) 36 dB (b) 40 dB (c) 45 dB. 45 dB represents the maximum power output level of the instrument.

was set at 36, 40, and 45 dB. The growth of the signal at 3.1 MHz and harmonics are plotted in Fig. 2, which demonstrates that at the highest power output level of 45 dB, the signal at the center frequency of 3.1 MHz is down approximately 1 dB from its expected value (assuming that each 1 dB increase in transmitted power would yield a 1 dB increase in measured signal). The second and third harmonics are, respectively, 10 and 17 dB below the fundamental at the highest power output. These data agree quite well with the theoretical description of $\sigma = 1$ conditions. The pressure waveforms measured at different source intensity levels are shown in Fig. 3. Some deviation from sinusoidal wave shape is evident at the 45 dB setting. To verify that the nonlinear effects were due to the medium and not generated by the shock excited output transducer, the waveforms were also measured at shorter ranges. At 45 dB power output and approximately 200 mm range, the magnitude of the spectrum at 3.1 MHz had dropped by approximately 10 dB (compared to the signal measured at 345 mm range), but the harmonic compo-

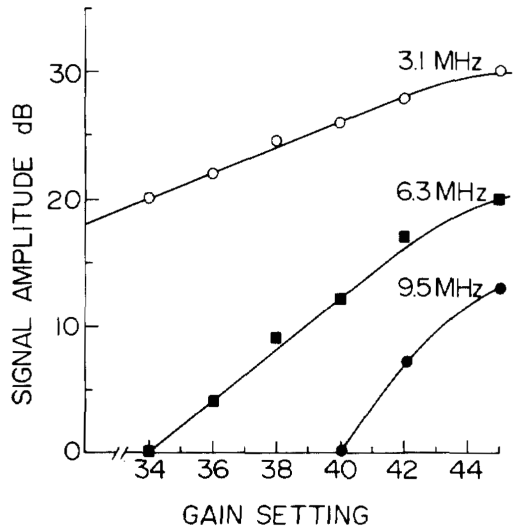

Fig. 2. Graph of the spectral magnitude (in dB above noise) versus transducer output power level (in dB) for signal components at 3.1, 6.3, and 9.5 MHz. The relative signal strengths at highest power output, 45 dB, are close to the theoretical description of $\sigma = 1$ weak shock conditions.

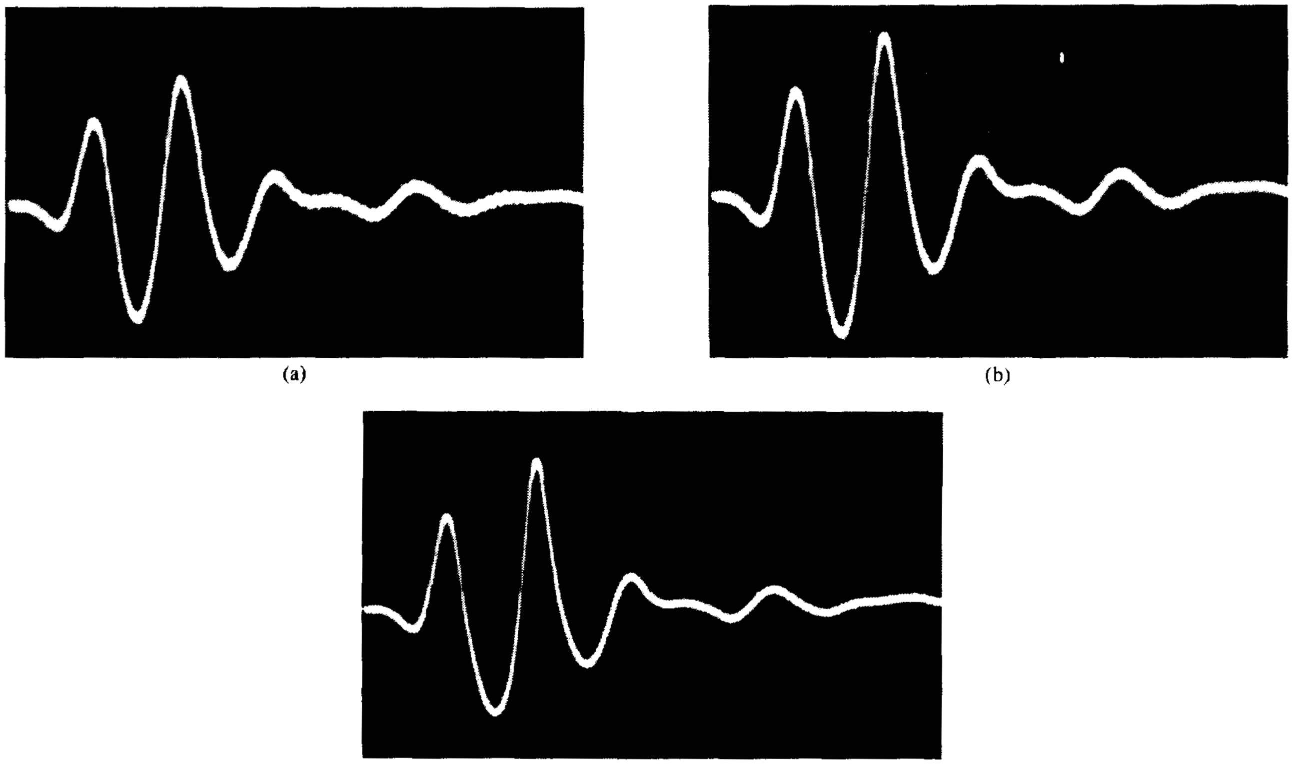

(a) (b) (c)

Fig. 3. Pressure waveforms near the focal region, at increasing power output levels. Horizontal scale: 0.2 μsec/div. Output power levels are (a) 36 dB, vertical scale 2 mV/div. (b) 39 dB, vertical scale adjusted between 2 and 5 mV/div. (c) 45 dB, vertical scale 5 mV/div.

nents were at or below the noise floor. Thus the observed acoustic field could not be described by the linear superposition of a signal and harmonics originating from the transmitter, even accounting for a smaller focal region and higher focal gain of the second harmonic assuming linear, diffraction limited focusing.

Other calculations support the case for observation of $\sigma = 1$ shock conditions. The engineering specifications for the Octoson [7] quote a typical maximum acoustic output of 4 μJ/pulse. Assuming this energy is transmitted over a pulse length of 1 μs, and is uniformly output over the full surface area of the transducer, a pulse averaged source intensity of $I_s = 0.11$ W/cm^2 is obtained. This is a factor of two higher than the value predicted by theory for

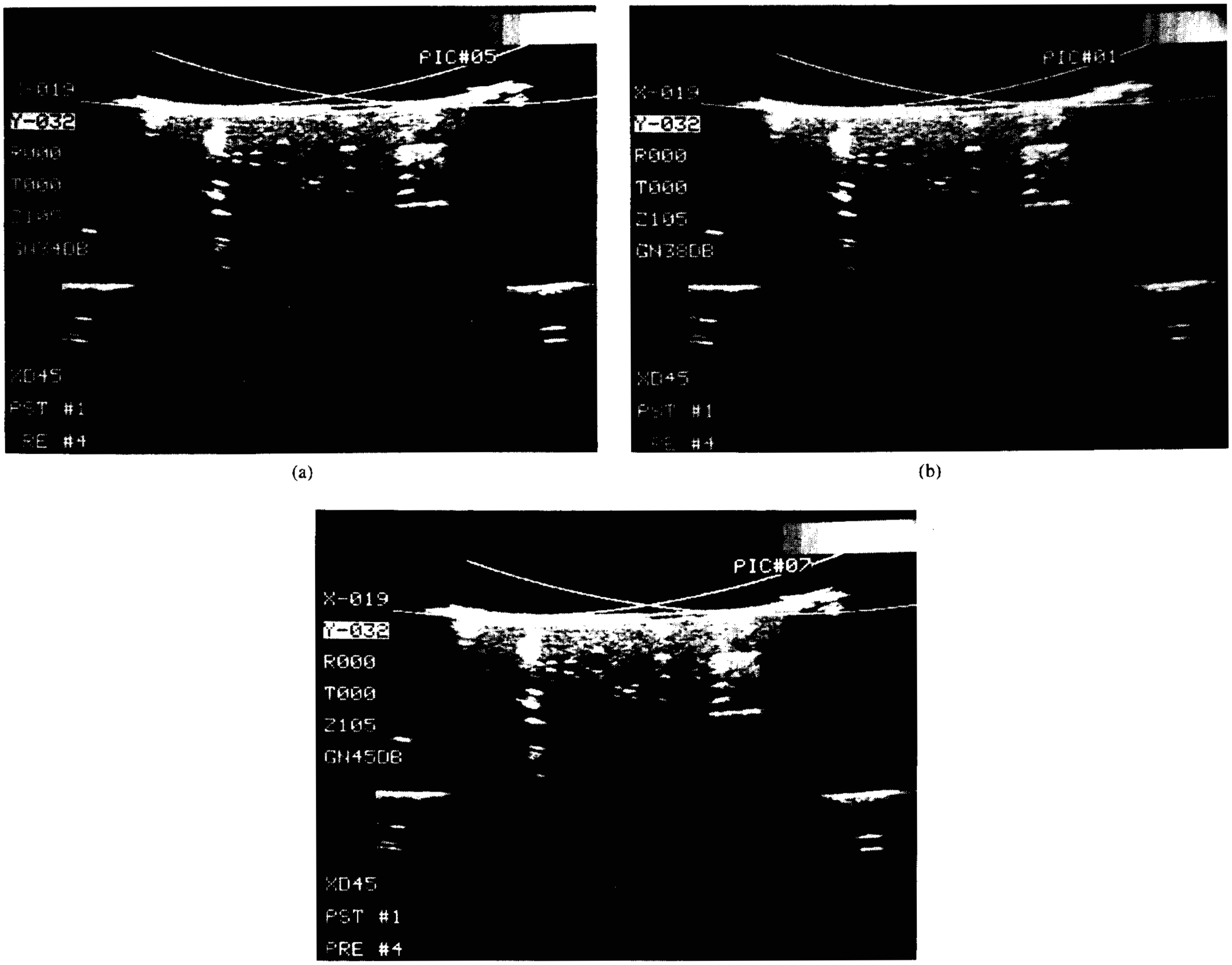

(a) (b) (c)

Fig. 4. Compound *B*-scan images of a phantom containing internal targets, taken at increasing power levels. TGC values are flat over the entire scan, but are adjusted to compensate for the change in power levels between scans. Output levels are (a) 34 dB (b) 38 dB (c) 45 dB.

weak shock production. However, the quoted value was not verified in this study, and the theory used in these calculations neglects any attenuation losses within the water path, neglects the broad band nature of the transmitted pulse, and does not account for beam diffraction effects, which are especially important near the focus. However, the theory is useful in providing an estimate of the source levels required to initiate finite amplitude distortion. Additional derivations have recently been presented to account for attenuation losses [11] and beam diffraction effects [12].

The effects of weak shock formation on image quality were assessed by comparing *B*-scan images obtained at different power outputs. Three effects of finite amplitude distortion could be considered to degrade image quality: a saturation effect where increasing power does not increase picture brightness, a lateral resolution reduction caused by beam broadening, and increased apparent attenuation, as energy converted to higher harmonics would be highly attenuated in the medium. To determine the presence or absence of these effects, images of a phantom containing targets were made at power output levels of 34, 38, and 45 dB. A flat transmit gain control (TGC) curve was used, but the level was adjusted in each case to produce a standard grey scale brightness in the first few millimeters of each image. Fig. 4 shows compound images produced using two transducers with focal regions positioned near the surface of the phantom. Only in the highest power output image (45 dB) is significant energy at higher harmonics incident on the phantom. A close inspection of targets within the phantom reveals that the lateral resolution is not degraded in the high power, weak shock case. Also, the apparent attenuation in each of the images is nearly identical. This would indicate that signal reduction caused by attenuation within the phantom, and beam broadening beyond the focal region, limits the production of additional finite amplitude effects. The system, in effect, has returned to linear conditions. A slight saturation effect occurs at higher power levels, however. The transmit gain control level in the above experiments was adjusted to compensate for power output, in order to maintain uniform image brightness. In a related set of experiments, the change in transmit gain control levels between 42 and 45 dB output settings was found to be less than the required change between 34 and 37 dB. However, since the transmit gain control amplifiers have nonlinear compression characteristics [8], this comparison is not exact. A detailed analysis of the RF signal received by the transducer under varying power output conditions would be required to quantify saturation effects.

Discussion and Conclusion

Acoustic weak shock conditions ($\sigma = 1$) are found at highest output power levels near the focal region of a commercially available *B*-scan imaging instrument. The onset of finite amplitude distortion is predicted by theory at these power levels for the center frequency and path length used. Operation at weak shock conditions does not appear to affect image quality. Presumably, the system is returned to linear conditions over a short propagation path in an attenuating medium, particularly where beam divergence is also acting to decrease the pressure amplitude. The theory shows in a straightforward manner that conversion of the 3 MHz Octoson system to the new 4 MHz instrument, coupled with increased transmit power required to overcome higher attenuation, would correspondingly increase the shock parameter. Of course, the nonlinear distortion could be drastically lowered by propagation through an attenuating medium, such as liver or kidney tissue [11]. However, some uses of the Octoson where the path between transducer and target (presumably located near the focal region for optimal resolution) does not include a long, attenuating, intervening tissue layer include examinations of the testicles and breasts, and imaging through amniotic fluid or the filled bladder. Presumably in these cases, a clinician utilizing a 3 or 4 MHz Octoson system would not require highest power levels to obtain a "bright" image, since the total attenuation would be small in comparison to deep penetration of the abdomen. In addition, any beam broadening and saturation effects should act to degrade image quality under hard shock conditions, again favoring selection of lower power levels for imaging. Thus, while the Octoson is capable of producing finite amplitude effects in water at highest power outputs, it is unlikely that weak shock conditions are present near the focal region in routine clinical examinations.

Acknowledgment

Thanks are due to Professor R. C. Waag and Professor E. L. Carstensen for their helpful discussions.

References

[1] T. G. Muir and E. L. Carstensen, "Prediction of nonlinear acoustic effects at biomedical frequencies and intensities," *Ultras. Med. Biol.*, vol. 6, pp. 345-357, 1980.
[2] E. L. Carstensen, W. K. Law, N. D. McKay, and T. G. Muir, "Demonstration of nonlinear acoustical effects at biomedical frequencies and intensities," *Ultras. Med. Biol.*, vol. 6, pp. 359-368, 1980.
[3] E. L. Carstensen, N. D. McKay, D. Delecki, and T. G. Muir, "Absorption of finite amplitude ultrasound in tissues," *Acoustics*, vol. 51, no. 2, pp. 116-123, 1982.
[4] F. Dunn, W. K. Law, and L. A. Frizzell, "Nonlinear ultrasonic wave propagation in biological materials," in *Proc. IEEE Ultrason. Symp.*, vol. 1, pp. 527-532, 1981.
[5] F. A. Duck and H. C. Starritt, "Acoustic shock generation by ultrasonic imaging equipment," *Br. J. Radiol.*, vol. 57, pp. 231-240, 1984.
[6] D. R. Bacon, "Finite amplitude distortion of the pulsed fields used in diagnostic ultrasound," *Ultras. Med. Biol.*, vol. 10, no. 2, pp. 189-195, 1984.
[7] Octoson specifications provided by Ausonics Corporation, 2915 South 160th Street, New Berlin, Wisconsin 53151, U.S.A.
[8] K. J. Parker and R. C. Waag, "Measurement of ultrasonic attenuation within regions selected from B-scan images," *IEEE Trans. Biomed. Eng.*, vol. BME-30, no. 8, pp. 431-437, 1983.
[9] P. A. Lewin, "Miniature piezoelectric polymer ultrasonic hydrophone probes," *Ultrasonics*, vol. 19, pp. 213-216, 1981.
[10] J. A. Shooter, T. G. Muir, and D. T. Blackstock, "Acoustic saturation of spherical waves in water," *J. Acoust. Soc. Am.*, vol. 55, no. 1, pp. 54-62, 1974.
[11] M. E. Haran and B. D. Cook, "Distortion of finite amplitude ultrasound in lossy media," *J. Acoust. Soc. Am.*, vol. 73, no. 3, pp. 774-779, 1983.
[12] B. G. Lucas and T. G. Muir, "Field of a finite-amplitude focusing source," *J. Acoust. Soc. Am.*, vol. 74, no. 5, pp. 1522-1528, 1983.

Kevin J. Parker (S'79-M'81) was born in Rochester, NY, in 1954. He received the B.S. degree in engineering science from the State University of New York at Buffalo in 1976 and the M.S. and Ph.D. degrees in electrical engineering from the Massachusetts Institute of Technology, Cambridge, in 1978 and 1981, respectively, with doctoral research on ultrasonic hyperthermia performed at the Laboratory for Medical Ultrasound.

Since joining the faculty at the University of Rochester, Rochester, NY, his research activities have concentrated on tissue characterization using ultrasound.

Dr. Parker is a member of the Acoustical Society of America.